

¹Feng Zhang
² Li Zhang
³ Yanshuang Xie
^{4*} Yaozhao Zhong
⁵ Lei Wang
⁶ Peitu Lin

Enhanced Typhoon-Induced Design Wave Height Estimation for Ocean Engineering Applications Using High Performance Computing



Abstract: - Coastal construction heavily depends on accurately estimating design wave parameters. This paper presents a technique for calculating ocean engineering design wave heights that addresses the challenges of inadequate wind speed and measured wave data in the field using High Performance Computing (HPC). The proposed method combines the Simulating WAVes Nearshore (SWAN) wave model driven by wind with two different wind field models: the NCEP/NCAR reanalysis wind field and the Jelesnianski typhoon model wind field. By combining these models, the study reduces the underestimation of wind speed and inaccurate depiction of typhoon-related details. The method's effectiveness is demonstrated by applying it to calculate the design wave elements of the deep-sea breeding platform in Dongluo Island, Fujian. The study results show that the platform can experience a maximum wave height of 9.42 m during a 50-year recurrence period. The research shows that the platform's southwest corner is the most vulnerable location. This new calculation method is a significant improvement in ocean engineering design since it overcomes the limitations that come with the lack of wind speed and measured waves. By utilizing multiple wind field models, the calculated wave heights' accuracy and reliability is considerably enhanced. The application of this method to the breeding platform in Dongluo Island has yielded valuable insights for designing resilient structures in similar oceanic environments. This study demonstrates the important application of computational numerical simulations in the field of ocean engineering, providing high-precision predictive capabilities for structural design and risk assessment.

Keywords: Numerical Simulation; SWAN; Reanalysis Big Data; Wave Height Design; Wave Elements

I. INTRODUCTION

In an era where computational capabilities are advancing rapidly, the intersection of ocean engineering and computer science offers unprecedented opportunities. Waves are one of the primary dynamic elements in the ocean. Komen [1] provide a comprehensive text on the dynamics and modeling of ocean waves, offering insights into the physics governing wave movement and the techniques used to model wave behavior. Donelan [2] delve into the nature of directional wave spectra, which characterize the distribution of wave energy across different directions and frequencies. Young [3] is concerned with wind-generated ocean waves. This work discusses the mechanisms through which wind transfers energy to the surface of the ocean to generate waves. Janssen's [4] discusses the complex interaction between ocean waves and the wind. Petruskas and Aagaard [5] discuss a method for extrapolating historical storm data to determine design wave heights in their paper. Goda [6] proposes a method for regional analysis of extreme wave height distribution. Mohan [7] discusses recent advances in the design and assessment of structures in the coastal zone. Suh [8] investigate the empirical simulation technique (EST) as a method to estimate design wave height. Wang [9] propose a new model specifically tailored for calculating design wave height in sea areas affected by typhoons. Panchang [10] focus on the extreme wave heights in the area of the Gulf of Mexico, a region where there is extensive offshore engineering activity. A novel method using a double entropy joint distribution function is introduced by Liu [11]. This application aims to refine the calculation of the design wave height. It emphasizes the stochastic nature of wave generation and propagation. Common methods for estimating design wave parameters in marine engineering include empirical wave formula-based methods [12], methods based on the correlation analysis of measured wind speed and waves [13], and mathematical calculation methods based on numerical wave models [14]. It is worth noting that artificial

¹ Fuzhou Institute of Oceanography, Minjiang University, Fuzhou 350000, China; Fujian Key Laboratory of Autonomous Controllable Software, Linewell Software Co., Ltd. Quanzhou, 362000, Fujian, China.

² Fujian Provincial Key Laboratory of Environmental Engineering, Fujian Provincial Academy of Environmental Science, Fuzhou 350000, China.

³ College of Ocean and Earth Science, Xiamen University, Xiamen 361005, China.

⁴ Fuzhou Institute of Oceanography, Minjiang University, Fuzhou 350000, China.

⁵ College of Mathematics and Statistics, Sichuan University of Science & Engineering, Yibin, 644000, China

⁶ Fujian Key Laboratory of Autonomous Controllable Software, Linewell Software Co., Ltd. Quanzhou, 362000, Fujian, China.

*Corresponding author: Yaozhao Zhong

Copyright © JES 2024 on-line : journal.esrgroups.org

intelligence has also been applied to the estimation of design wave heights. Alexandre [15] present a hybrid approach combining genetic algorithms with extreme learning machines to reconstruct significant wave heights accurately. Fan [16] develops a novel Long Short-Term Memory (LSTM)-based model to predict significant wave height. Continuing the trend in AI, Gao [17] provides insight into the ability of advanced machine learning models to handle the complex dynamics of wave behaviour by tuning an LSTM neural network to predict wave heights. Afzal [18] explore significant wave height prediction using various machine learning techniques. By focusing on extreme wave analysis, the research holds potential for enhancing safety measures and risk assessment in marine and coastal engineering.

With the development of computer numerical calculations, numerical model-based methods have become the preferred choice for wave calculations due to their speed, intuitiveness, and accuracy. The development of numerical wave calculations has gone through three generations. The most commonly used wave calculation models fall into three primary categories.: first, the shallow water equation-based wave calculation models, which have limited numerical simulation accuracy in areas with rapid seabed topography changes and shallow water depth; second, the energy balance equation-based wave calculation models, with SWAN being the representative model, which is widely applied and offers good simulation accuracy; third, wave calculation models based on the Boussinesq equation, with MIKE BW/SW as the representative model, which is suitable for small-scale wave calculations in complex terrains.

Liu [14] utilized the SWAN model to simulate wave processes in the sea area near the Rudong wind farm over the past 20 years driven by a combination of the WRF model wind field and the CCMP wind field. They obtained different return period wind speeds and wave parameters. Wen [19] nested the SWAN and WAVEWATCH III models to calculate the wave field in the vicinity of the Pearl River Estuary for a 20-year period driven by the WRF model wind field. They used the Gumbel extreme value function to compute the 50-year and 100-year return period wave extremes in that area. Qi [20] employed the MIKE SW model to reproduce the wave variations in the Lianyungang Sea area during the passage of Typhoon 0713 driven by the WRF model wind field. Yuan [21] utilized the MIKE21 SW model to calculate the design wave parameters in that region driven by design wind speeds from meteorological stations near the Yangtze River Estuary.

This paper introduces ocean model, a novel approach integrating high-performance computing with advanced wave modeling techniques to revolutionize ocean engineering design. Through the fusion of multiple wind field models, it significantly enhances the accuracy and reliability of calculated wave heights, ultimately leading to structures in challenging oceanic environments. The model is powered by wind fields from the NCEP reanalysis and the Jelesnianski typhoon model. The methodology is demonstrated using a deep-sea aquaculture platform project near Dongluo Island in Lianjiang County, Fujian Province, China. This study demonstrates the important application of computational numerical simulations in the field of ocean engineering, providing high-precision predictive capabilities for structural design and risk assessment.

II. NUMERICAL MODEL AND DATA

A. Research Area

The deep-sea aquaculture platform project in Dongluo Island, Lianjiang County, Fujian Province, is located in the northern part of the Beijiao Strait, within the waters southwest of Dongluo Island in the Taishi Town of Lianjiang County (Figure 1). The Beijiao Strait is situated north of Huangqi Peninsula and connects Luoyuan Bay Kemenkou and Sandu'ao. The aquaculture platform is bordered by Xiluo Island and Dongluo Island to the north, with a distance of only 500 meters from Dongluo Island. The Huangqi Peninsula lies about 5 kilometers to the south and approximately 3.5 kilometers to the east from the mainland coastline. The Beijiao Strait is characterized by numerous islands and reefs, and the water depth exhibits complex variations.



Figure 1: Project Engineering Location, Beijiao Marine Station, and Huangqi Buoy

According to the statistics from the Beijiao Meteorological and Oceanographic Station (Figure 1) in the "Hydrological and Climatic Records of the East China Sea Area" [22], the predominant wind direction in the region throughout the year is northeast, followed by east-northeast, and then southwest-south. The wind direction shows distinct seasonal variations, with northeast winds being the most frequent during autumn and winter. In spring, both northeast and east-northeast winds are common, while southwest-south winds are most prevalent during summer.

Based on the hourly wind speed statistics from Beijiao during the period of 1982-2001, the average wind speeds range from 4.4 to 6.3 m/s, with the highest values occurring in October and November, and the lowest in May. The highest recorded wind speed is 37.0 m/s, recorded during the 2001 Typhoon Feiyan. The long-term average wave height at Beijiao station is 1.5 m, with annual average wave heights ranging from 1.2 to 1.7 m. The maximum wave heights in a year are no less than 4.5 m, with most occurrences happening during the typhoon-influenced season from July to October.

B. SWAN Model

SWAN is a 3rd generation coastal wave model from Delft University, Netherlands. It is suitable for computing wind waves, swells, and mixed waves in shallow water and nearshore areas.

The SWAN model employs the spectral balance equation to describe the generation and evolution of waves in the nearshore region. In a Cartesian coordinate system, the spectral balance formula is as follows:

$$\frac{\partial N}{\partial t} + \frac{\partial(C_x N)}{\partial x} + \frac{\partial(C_y N)}{\partial y} + \frac{\partial(C_\sigma N)}{\partial \sigma} + \frac{\partial(C_\theta N)}{\partial \theta} = \frac{S}{\sigma} \tag{1}$$

In the equation: N represents the spectral density (Joule/m²/Hz); t represents time (s); σ represents the wave frequency (Hz); Theta (θ) denotes the direction in which the wave propagates, which is always perpendicular to the direction of the wave crest. n; C_x and C_y represent the wave propagation velocity components in the x and y directions, the expression is as follows:

$$C_x = \frac{1}{2} \left[1 + \frac{2kd}{\sinh(2kd)} \right] \frac{\sigma k_x}{k^2} + U_x \tag{2}$$

$$C_y = \frac{1}{2} \left[1 + \frac{2kd}{\sinh(2kd)} \right] \frac{\sigma k_y}{k^2} + U_y \tag{3}$$

k_x and k_y represent the directional wave numbers; d represent the water depth (m); U_x and U_y represent the components of the flow velocity in the x and y directions, respectively (m/s); C_σ and C_θ represent the components of the wave propagation velocity in the spectral space (σ, θ) (m/s). Here are the expressions:

$$C_\sigma = \frac{\partial \sigma}{\partial d} \left[\frac{\partial d}{\partial t} + \vec{U} \cdot \nabla d \right] - C_\sigma \vec{k} \cdot \frac{\partial \vec{U}}{\partial s} \tag{4}$$

$$C_\theta = \frac{1}{k} \left[\frac{\partial \sigma}{\partial t} \frac{\partial d}{\partial m} + \vec{k} \cdot \frac{\partial \vec{U}}{\partial m} \right] \tag{5}$$

In the equation, C_g represents the wave group velocity (m/s); s represents the spatial coordinate along the θ direction; m represents the coordinate perpendicular to s; S indicates the source-sink term, which encompasses all physical processes capable of diminishing, redistributing and generating wave energy.

C. Calculation range and mesh grid

To avoid limitations in wave growth and propagation due to a small calculation domain, and considering that the predominant wave direction in the project area is northeast-north, the design wave model covers a calculation range of 24.8°-27.4°N, 118.8°-123°E. The model uses a triangular grid to discretize the calculation domain, with a gradual increase in grid resolution from the ocean boundary towards the coastline. The grid is further refined

near the project area, with a minimum grid edge length of approximately 30m (Figure 2). The calculation domain consists of a total of 18,522 grid cells, accurately capturing the complex and variable coastline and islands. The water depth data in the project area is based on measured depths, while nearshore regions utilize a fusion of data from nautical charts, remote sensing, and other sources. For the outer regions, interpolated water depth data from the etop2-1min dataset is used.

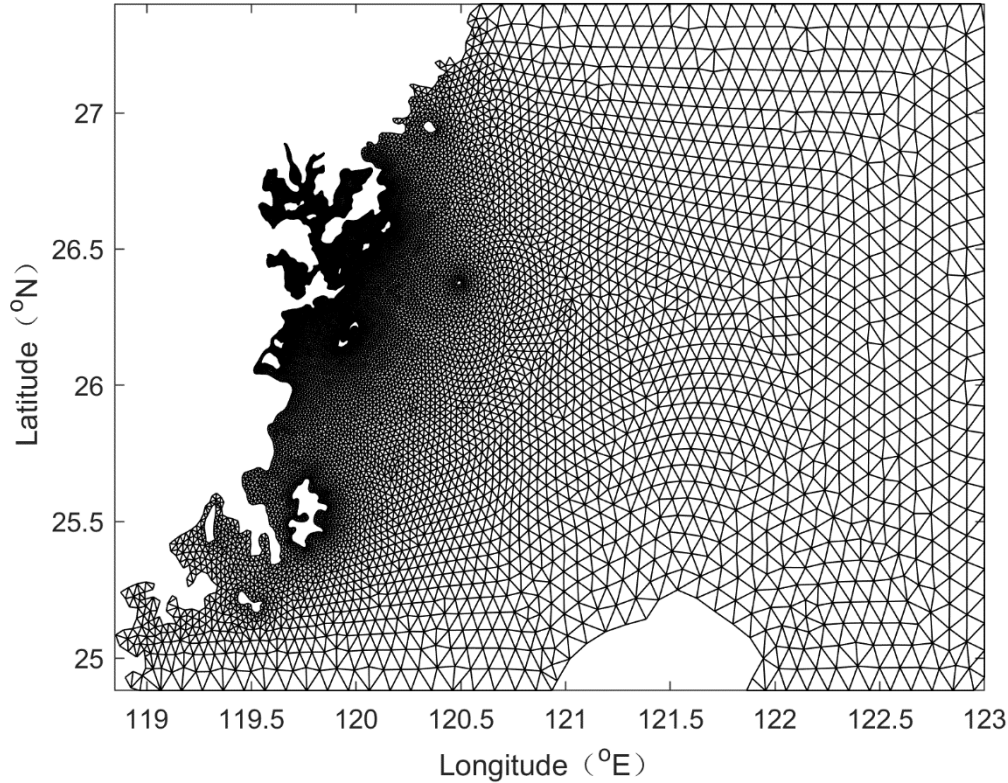


Figure 2: Distribution of the Computational Domain Grid

D. NCEP/NCAR Reanalysis Wind Field

The National Centers for Environmental Prediction and the National Center for Atmospheric Research jointly produce the NCEP/NCAR reanalysis dataset. The system uses a global data assimilation process and extensive databases to ensure quality control and effectively integrate data from multiple sources, including surface, ship, radiosonde, wind profiler, aircraft, and satellite measurements. The NCEP/NCAR reanalysis wind field data covers the entire globe and consists of a grid with a resolution of 192*94 points. In this study, daily four-times NCEP/NCAR reanalysis wind field data from 2000 to 2020, spanning a period of 20 years, were selected for the study area.

E. Jelesnianski Typhoon Model Wind Field

Typhoon waves have a significant impact on the study area in this paper, and the highest wave heights in this region are often associated with typhoon influences. Therefore, more accurate calculations of wave heights are required during typhoon events. During typhoons, the structure of the cyclonic wind field undergoes rapid changes that the NCEP wind field accuracy is insufficient to capture. Hence, the Jelesnianski wind field is used to reanalyze the wind fields of 47 significant typhoon events that occurred between 2000 and 2020 and had a notable impact on the engineering area. The Jelesnianski wind field expresses the wind speed profile using the maximum wind speed and is represented by the following expression:

$$V_R = V_{Rmax} \frac{2\left(\frac{r}{R_{max}}\right)}{1+\left(\frac{r}{R_{max}}\right)^2} \tag{6}$$

In the equation, V_R represents the typhoon circulation wind speed (m/s) at a distance r from the typhoon center; V_{Rmax} represents the maximum circulation wind speed (m/s); R_{max} represents the radius (m) at which the maximum circulation wind speed is measured from the typhoon center.

III. METHOD AND RESULTS

A. Model Applicability Verification

To verify the accuracy of wave calculations, two typhoon events, Typhoon Sudilo (1513) and Typhoon Dujuan (1521) in 2015, were selected for wave calculation validation. The Huangqi Ocean Monitoring Buoy, located approximately 2 km southeast of the project site (Figure 1), was used to compare the model results with the measured significant wave heights at the buoy. This comparison was used to assess the applicability of the model in this marine area and calibrate the model's wave calculation parameters.

Typhoon Sudilo (1513) originated on the northwest Pacific Ocean on July 30, 2015, and gradually intensified. It reached its peak intensity of Category 17 or higher on August 3. On the morning of August 8, it made landfall in Hualien City, Taiwan, with maximum winds near the center reaching 15 on the Beaufort scale. Later that evening, it made landfall in Putian City, Fujian Province, China, with maximum winds near the center reaching 13 on the Beaufort scale.

Typhoon Dujuan (1521) formed on September 23, 2015, in the northwest Pacific Ocean. It was named Dujuan and was upgraded to a moderate typhoon on the 25th. On the 26th, it encountered dry air and intensified into a strong typhoon. On the 27th, it further intensified into a super typhoon. It made landfall in Taiwan on the 28th and landed in Xiuyu District, Putian City, Fujian Province, China, on the 29th.

From Figures 3 and 4, it can be observed that the simulated wave results at the Huangqi buoy location during both typhoon events generally match the measured data well, especially in accurately capturing the peak significant wave height. Based on the buoy measurements, it can be seen that even when the typhoon was still far away, there were already typhoon waves of about 0.5m at the Huangqi buoy location, likely caused by the prevailing southwest monsoon during the summer. The typhoon wind field model used in this study does not include the influence of background winds such as the monsoon, which leads to underestimated wave heights when the typhoon is far away. Overall, the model designed in this study is feasible for numerical wave calculations in this marine area.

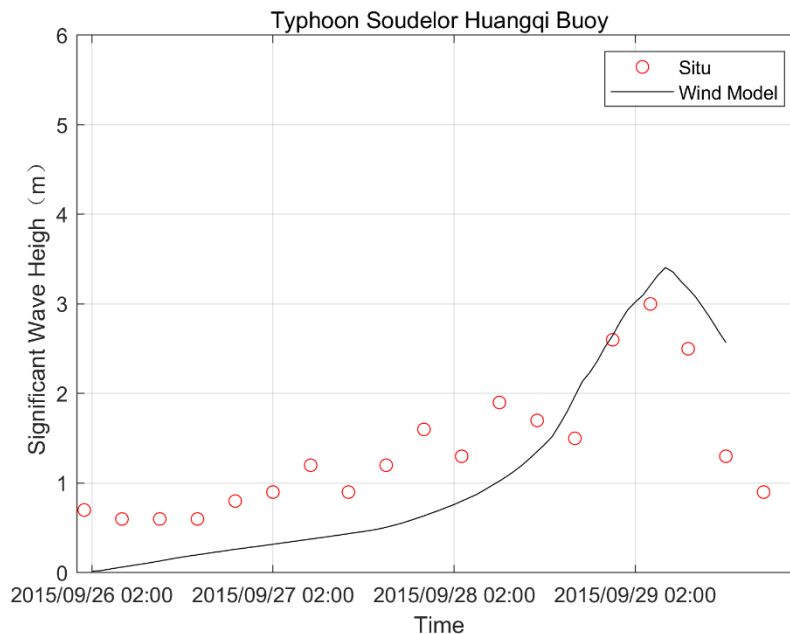


Figure 3: Verification of simulated significant wave height for Typhoon Soudelor

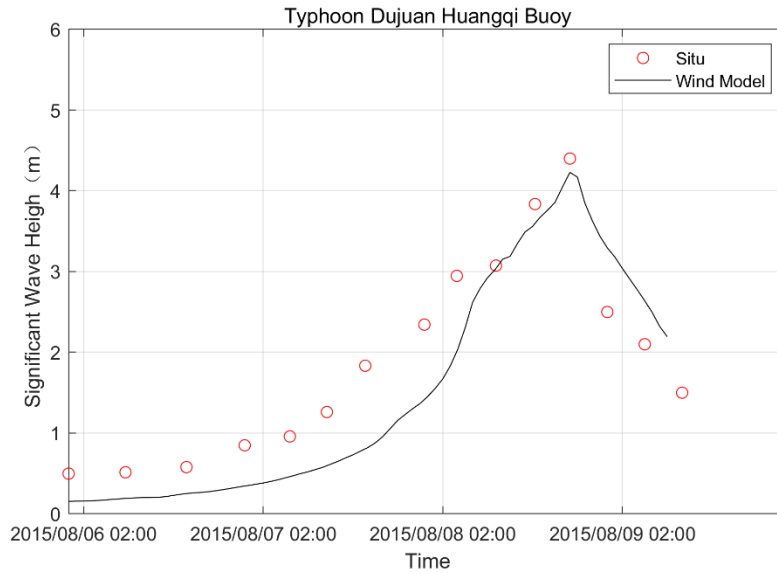


Figure 4: Verification of simulated significant wave height for Typhoon Dujan

B. 50-year Return Period Wind Speed Estimation

Based on the statistical analysis of 20 years (2000-2020) of NCEP/NCAR reanalysis wind data and 47 typhoon events with Jelesnianski wind data, the most frequently occurring wind direction at the location of the aquaculture platform is NE (40.0%), followed by E (16.1%), and then SW (11.1%). The return period wind speeds for various directions in the project area were calculated using the Gumbel distribution, as shown in Table 1. The return period curve for NE wind speeds is presented in Figure 5.

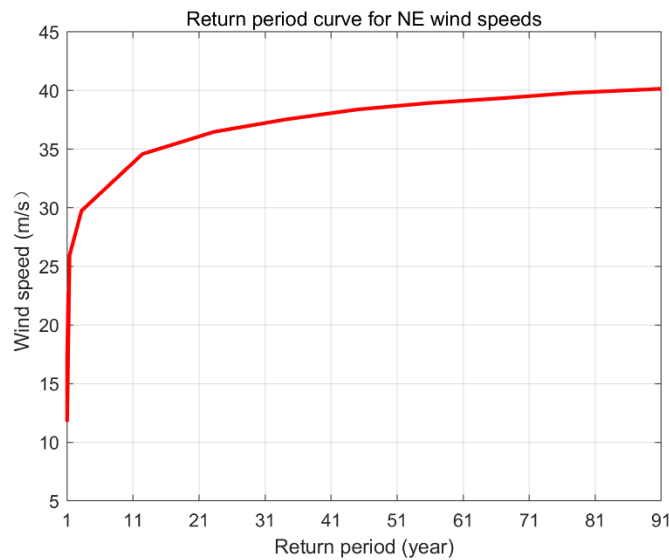


Figure 5: Return period curve for NE wind speeds

Table 1: Wind speed estimates for a 50-year return period.

Wind Direction	N	NE	E	SE	S	SW	W	NW
Wind Speed (m/s)	34.90	38.88	23.07	19.57	20.96	21.85	21.86	30.77
Frequency of Occurrence	9.1%	40.0%	16.1%	8.6%	10.8%	11.1%	2.8%	1.5%

C. Design Wave Parameters Calculation and Analysis

The SWAN model was used to perform 20 years of continuous wave calculations. The results show that the maximum calculated significant wave height for the fish farming platform over the 20-year period (2000-2020) is 4.75m, with a wave direction of 193o (towards the east-northeast, ENE direction), occurring on September 14, 2008, at 7:00 AM during the passage of Typhoon Senlak. The second-largest significant wave height is 4.73m,

with a wave direction of 196° (towards the east-northeast, ENE direction), occurring on August 9, 2009, at 9:00 AM during the passage of Typhoon Morakot.

Based on the calculations using the 50-year recurrence wind speed results, wave calculations were performed for eight uniformly distributed wind directions, and the following wave parameters were obtained for four selected locations on the fish farming platform (as shown in Figure 1 and Table 2): significant wave height, wave period, zero-crossing period, and spectral peak period, all provided on an hourly basis.

Table 2: Extracted Wave Parameters Locations

Index	Longitude	Latitude
1	119°53'28.196"	26°24'12.354"
2	119°54'08.420"	26°24'07.713"
3	119°54'10.096"	26°24'19.490"
4	119°53'29.789"	26°24'24.140"

Figure 6 demonstrates the significant wave height around the aquaculture platform, influenced by eight different wind directions, for a 50-year return period. The simulation shows that to the open sea's right of Dongluo Island, wave heights can surpass 8 meters. However, Dongluo Island along with Zhiluo and Xiluo Islands greatly diminishes wave height within the engineering zone. Wave heights are higher when affected by winds from the NE, N, E, SE, and NW. Conversely, the S, W, and SW winds result in smaller waves, likely due to the blocking effect of the Huangqi Peninsula. Dongluo and surrounding islands hinder wave propagation from NE, N, E, SE, and S winds, significantly reducing wave heights at the platform. The platform's southwestern corner is particularly susceptible to wind and wave impacts.

Table 3 contains statistical data on wave elements over a 50-year return period within the engineering area. The highest wave, influenced by northerly winds including N, NE, E, SE, SW, and W, occurs at the southeastern corner (Index 2). For southern winds, the peak significant wave height is at the northeast corner (Index 3), while the NW wind lifts the highest waves at the southwest corner (Index 1). The maximum height, reaching 9.42 meters at the southeastern corner (Index 2), is under the influence of NE wind for the same 50-year period.

Table 3: Wave Characteristics in the Engineering Area for a 50-year Return Period.

Wind Direction	Index	Significant Wave Height (m)	Maximum Wave Height (m)	Peak Wave Period (s)	Zero-Crossing Period (s)
N	1	3.43	6.55	5.62	5.17
	2	3.59	6.85	5.87	5.38
	3	3.10	5.91	5.35	4.89
	4	3.26	6.23	5.46	5.02
NE	1	4.24	8.09	6.63	6.06
	2	4.93	9.42	7.30	6.83
	3	3.60	6.87	6.26	5.56
	4	3.65	6.98	6.06	5.43
E	1	3.53	6.74	7.23	6.66
	2	4.14	7.90	7.77	7.39
	3	3.42	6.54	7.52	6.93
	4	3.18	6.07	6.92	6.19
SE	1	2.66	5.08	5.98	5.19
	2	3.10	5.93	6.76	6.06
	3	2.99	5.71	6.82	6.09
	4	2.61	4.98	5.98	5.15
S	1	1.96	3.75	4.49	3.87
	2	2.23	4.27	4.95	4.27
	3	2.27	4.34	5.14	4.44
	4	1.97	3.76	4.51	3.89
SW	1	1.24	2.38	3.19	2.54
	2	1.44	2.75	3.53	2.90
	3	1.42	2.70	3.55	2.86
	4	1.24	2.37	3.20	2.58
W	1	1.47	2.81	3.70	3.12
	2	1.49	2.85	3.70	3.10
	3	1.49	2.84	3.72	3.13
	4	1.47	2.82	3.69	3.09
NW	1	2.90	5.54	5.11	4.74
	2	2.85	5.45	5.06	4.69
	3	2.80	5.35	5.05	4.67
	4	2.87	5.48	5.10	4.73

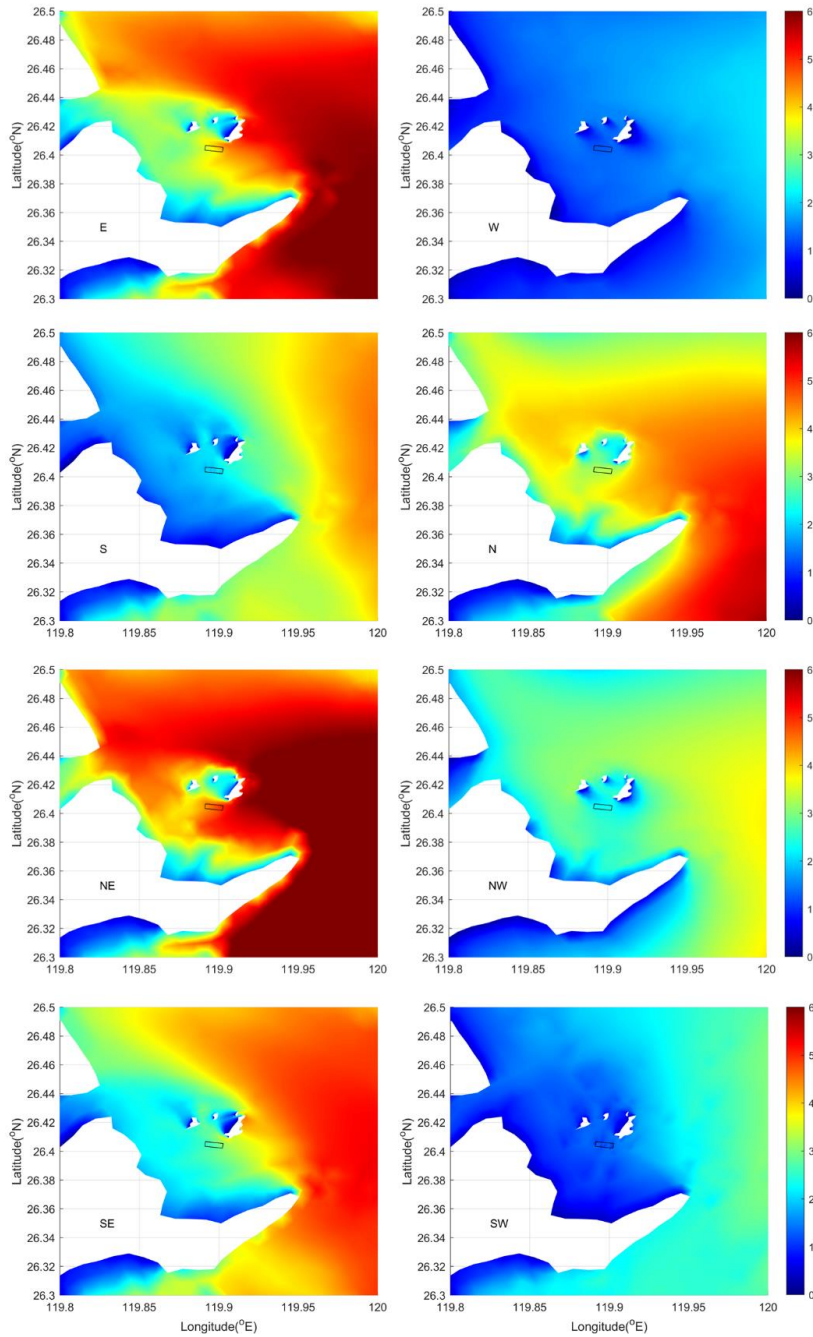


Figure 6: Distribution of Significant Wave Heights (m) for a 50-year Return Period in Eight Wind Directions.

IV. CONCLUSIONS

This paper presents a method for calculating ocean engineering design wave parameters based on the SWAN wave model, NCEP/NCAR reanalysis wind fields, and Jelesnianski typhoon wind fields. The method addresses the issue of lacking wind speed and wave measurements in typical marine engineering areas. It proposes using reanalysis wind fields and the Gumbel distribution method to estimate wind speeds for different return periods. Then, the SWAN model is used to simulate wave fields for each wind speed, resulting in the design wave parameters required for marine engineering construction. This methodology is applied to calculate the wave parameters for the deep-sea aquaculture platform near Dongluo Island in Fujian. The results show that the maximum of the wave height for a 50-year return period at the platform is 9.42 meters, and it is identified that the most dangerous location for the platform is its southwestern corner. This study demonstrates the important application of computational numerical simulations in the field of ocean engineering, providing high-precision predictive capabilities for structural design and risk assessment.

ACKNOWLEDGMENT

This study was supported by the Fujian Province Natural Science Foundation(No:2023J011573, 2023J011402), the Fujian science and technology Major special project(No:2022NZ033023), the Fujian Marine Economic Development Special Fund Project (No:FJHJF-L-2022-17), Fujian Province Key Science and Technology Innovation Project(2022G02009) and the MJU Scientific Research Foundation for Talents (No: MJY22033, MJY23014).

REFERENCES

- [1] Komen, G. J., Cavaleri, L., Donelan, M., Hasselmann, K., Hasselmann, S., & Janssen, P. A. E. M. (1996). Dynamics and modelling of ocean waves (p. 554).
- [2] Donelan, M. A., Hamilton, J., & Hui, W. (1985). Directional spectra of wind-generated ocean waves. *Philosophical Transactions of the Royal Society of London. Series A, Mathematical and Physical Sciences*, 315(1534), 509-562.
- [3] Young, Ian R. *Wind generated ocean waves*. Elsevier, 1999.
- [4] Janssen, Peter. *The interaction of ocean waves and wind*. Cambridge University Press, 2004.
- [5] Petruskas C, Aagaard P M. Extrapolation of historical storm data for estimating design-wave heights. *Society of Petroleum Engineers Journal*, 1971, 11(01): 23-37.
- [6] Goda, Yoshimi, et al. "Population distribution of extreme wave heights estimated through regional analysis." *Coastal Engineering* 2000. 2001. 1078-1091.
- [7] Mohan, Ram K., Orville Magoon, and Mark Pirrello, eds. "Advances in coastal structure design." *American Society of Civil Engineers*, 2003.
- [8] Suh K D, Kim M, Chun J. Estimation of design wave height using empirical simulation technique. *Ocean engineering*, 2013, 61: 39-49.
- [9] Wang L, Chen B, Zhang J, et al. A new model for calculating the design wave height in typhoon-affected sea areas. *Natural hazards*, 2013, 67: 129-143.
- [10] Panchang, Vijay, Chan Kwon Jeong, and Zeki Demirebilek. "Analyses of extreme wave heights in the Gulf of Mexico for offshore engineering applications." *Journal of Offshore Mechanics and Arctic Engineering* 135.3 (2013).
- [11] Liu G, Chen B, Jiang S, et al. Double entropy joint distribution function and its application in calculation of design wave height. *Entropy*, 2019, 21(1): 64.
- [12] Goda Y. Design wave height selection in intermediate-depth waters. *Coastal engineering*, 2012, 66: 3-7.
- [13] Wang L, Xu X, Liu G, et al. A new method to estimate wave height of specified return period. *Chinese Journal of Oceanology and Limnology*, 2017, 35: 1002-1009.
- [14] Liu G, Xu P, Kou Y, et al. Design wave height parameter estimation model reflecting the influence of typhoon time and space. *Journal of Marine Science and Engineering*, 2021, 9(9): 950.
- [15] Alexandre E, Cuadra L, Nieto-Borge J C, et al. A hybrid genetic algorithm extreme learning machine approach for accurate significant wave height reconstruction. *Ocean Modelling*, 2015, 92: 115-123.
- [16] Fan S, Xiao N, Dong S. A novel model to predict significant wave height based on long short-term memory network. *Ocean Engineering*, 2020, 205: 107298.
- [17] Gao S, Huang J, Li Y, et al. A forecasting model for wave heights based on a long short-term memory neural network. *Acta Oceanologica Sinica*, 2021, 40(1): 62-69.
- [18] Afzal M S, Kumar L, Chugh V, et al. Prediction of significant wave height using machine learning and its application to extreme wave analysis. *Journal of Earth System Science*, 2023, 132(2): 1-17.
- [19] Wen Xianhua, Wu Yi. Calculation of Extreme Waves in the Vicinity of the Pearl River Estuary. *Marine and Lake Sciences Bulletin*, 2018(6): 8.
- [20] Qi Qinghui. Numerical Simulation of Typhoon Waves in the Lianyungang Sea Area Based on WRF and MIKE-SW Models. *Water Transport Engineering*, 2015(7): 36-40.
- [21] Yuan Hua, Jia Xiao, Wan Yuanyang. Application of Spectrum Equation Model in the Calculation of Design Wave Parameters. *Waterway and Port*, 2013, 34(004): 293-296.
- [22] Sun Xiangping, Yao Jingxian. *Overview of Coastal Ocean Hydrology and Meteorology in China*. Science Press, 1981.